Insight into Serum Protein Interactions with Functionalized Magnetic Nanoparticles in Biological Media

Hilda T. R. Wiogo,[†] May Lim,[†] Volga Bulmus,[‡] Lucía Gutiérrez,[§] Robert C. Woodward,[§] and Rose Amal*[,†]
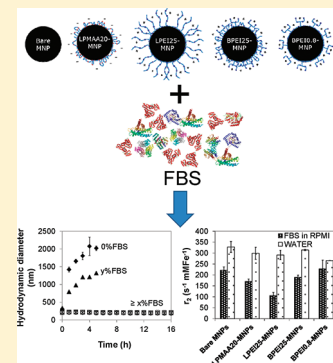
[†]ARC Centre of Excellence for Functional Nanomaterials, School of Chemical Engineering, University of New South Wales, Sydney NSW 2052, Australia

[‡]Department of Chemical Engineering, İzmir Institute of Technology, Gülbahçe Urla 35430, Turkey

[§]School of Physics, The University of Western Australia, Crawley WA 6009, Australia

Ⓢ *Supporting Information*

ABSTRACT: Surface modification with linear polymethacrylic acid (20 kDa), linear and branched polyethylenimine (25 kDa), and branched oligoethylenimine (800 Da) is commonly used to improve the function of magnetite nanoparticles (MNPs) in many biomedical applications. These polymers were shown herein to have different adsorption capacity and anticipated conformations on the surface of MNPs due to differences in their functional groups, architectures, and molecular weight. This in turn affects the interaction of MNPs surfaces with biological serum proteins (fetal bovine serum). MNPs coated with 25 kDa branched polyethylenimine were found to attract the highest amount of serum protein while MNPs coated with 20 kDa linear polymethacrylic acid adsorbed the least. The type and amount of protein adsorbed, and the surface conformation of the polymer was shown to affect the size stability of the MNPs in a model biological media (RPMI-1640). A moderate reduction in r_2 relaxivity was also observed for MNPs suspended in RPMI-1640 containing serum protein compared to the same particles suspended in water. However, the relaxivities following protein adsorption are still relatively high making the use of these polymer-coated MNPs as Magnetic Resonance Imaging (MRI) contrast agents feasible. This work shows that through judicious selection of functionalization polymers and elucidation of the factors governing the stabilization mechanism, the design of nanoparticles for applications in biologically relevant conditions can be improved.

■ INTRODUCTION

Magnetic nanoparticles have many applications in biomedical technologies, such as Magnetic Resonance Imaging,[1] magnetic separation,[2] hyperthermia,[3] sensing,[4] and drug[5] or gene delivery.[6] Applications have dramatically increased in the past decade due to their unique combination of physical and chemical properties. Magnetite nanoparticles (MNPs), in particular, are of great interest as they are easily produced, possess good magnetic properties, and are nontoxic and biodegradable.

In any in vivo biomedical application, particle size stability is a key criterion. Large nanoparticle aggregates (>4 μm) are more likely to create life-threatening blockages in the blood vessels or the capillary bed of the lungs. The particles may also be filtered (depending on their size) by the body's immune system.[7] Particles injected intravenously are cleared predominantly by the liver (Kupffer cells) and spleen macrophages, with particles larger than 200 nm being cleared faster by Kupffer cells than their smaller counterparts.[8] Smaller particles (10 to 20 nm) are captured and eliminated rapidly by the liver, while particles with a hydrodynamic diameter below 6 nm are cleared rapidly by the kidney.[9] Hence it is desirable to maintain a hydrodynamic diameter of particles between 30 and 150 nm to ensure a longer circulation time within the body.

Functionalization of the MNPs surface with appropriate polymeric molecules to improve and maintain their size stability, as well as to provide appropriate functional groups for interaction-based applications, is therefore an important step in the design of MNPs for biomedical applications.[10] The functionalization of magnetite nanoparticles with polyelectrolytes such as polymethacrylic acid and polyethylenimine is of particular interest in biomedical applications. Due to the abundance of the carboxylic acid (−COOH) group on its polymer backbone (Figure 1a), polymethacrylic acid is commonly used to conjugate and bind other molecules of interest to the surface of the magnetic nanoparticles.[11−13] Polyethylenimine, in contrast, has been used to deliver oligonucleotides or DNA in gene therapy.[14] Due to the abundance of secondary amines (=NH) on the linear polyethylenimine molecules, and primary, secondary, and tertiary amines (−NH₂, =NH, and ≡N) on branched
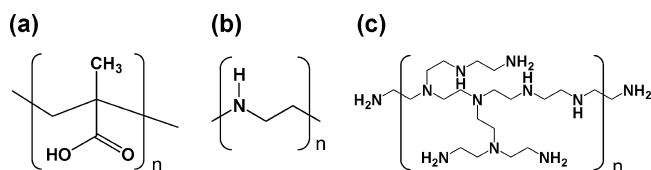
Figure 1. Structure of (a) linear polymethacrylic acid, (b) linear poyethylenimine, and (c) branched polyethylenimine.

polyethylenimine (Figure 1b,c), polyethylenimines can electrostatically bind with DNA and then release them once inside cells via polymer-induced osmotic swelling.[6,14−16]

An equally important consideration in the particle design is the unavoidable interaction between the magnetic nanoparticles and serum proteins that are ubiquitous in the biological environment. The effect of serum protein adsorption on the behavior of various nanoparticles in a biological system has been studied often, with many investigations focusing on the effect on cell uptake and cytotoxicity of the particles.[17] Reports in the literature have shown that serum protein adsorption can influence the aggregation behavior of nanoparticles in biologically relevant media, depending on the particles' characteristics, including shape and curvature, porosity and crystallinity, roughness, polymer coating, hydrophobicity or hydrophilicity, and types of suspension media.[18−24] It can either reduce or exacerbate the aggregation of nanoparticles. However, the exact mechanisms behind protein adsorption and their stabilization effects have not been fully elucidated. Thus, further systematic and in-depth study on the bionanoparticles interaction and factors that influence aggregation stability of MNPs in biological media is required in order to better design and tailor nanoparticles for different applications.

The present study investigates serum protein adsorption onto magnetite nanoparticles that were functionalized with negatively charged polymethacrylic acid or positively charged polyethylenimine. Ethylenimine polymers with different molecular architecture (branched or linear) and molecular weights were used. A cell culture media, RPMI-1640, was used to mimic the properties of biological media, and fetal bovine serum (FBS), which consists of a complex mixture of proteins, electrolytes, antibodies, antigens, and hormones, was added as a model biological serum to mimic the biological components in biological fluid. The functionalized-MNPs were characterized by Fourier Transform Infrared Spectroscopy (FTIR), thermogravimetric analysis (TGA), dynamic light scattering (DLS), and ζ potential analysis. The formation of protein corona on MNPs surfaces was visualized by Transmission Electron Microscopy (TEM) and studied by 1-D Sodium Dodecyl Sulfate−Polyacrylamide Gel Electrophoresis (SDS-PAGE). The amount of adsorbed protein was quantified by using a Bradford assay and then identified by using Liquid Chromatography−Mass Spectrometry/Mass Spectrometry (LC-MS/MS). The impact of protein interactions with functionalized MNPs on the biological function of nanoparticles was assessed by the size measurement in biological media by using DLS. The effect on the MNPs relaxivity was then determined by proton relaxometry to study the potential of the functionalized MNPs as MRI contrast agents.

■ EXPERIMENTAL SECTION

Materials. Ferrous chloride tetrahydrate (FeCl$_2$·4H$_2$O), Ferric chloride hexahydrate (FeCl$_3$·6H$_2$O), methacrylic acid, 4-cyano-4-(phenylcarbonothioylthio)pentanoic acid, 4,4′-azobis(4-cyanovaleric

acid), and bovine serum albumin (BSA) were obtained from Sigma-Aldrich. Sodium hydroxide (NaOH) and hydrochloric acid (HCl) were obtained from Ajax Finechem. Linear polyethylenimine (LPEI25, M_w = 25 000) was obtained from Polysciences, while branched polyethylenimine (BPEI0.8, M_w = 0.8 kDa, and BPEI25, M_w = 25 000 Da) was purchased from Sigma-Aldrich. Biological media, RPMI-1640 (Cat no. 21870-092), and fetal bovine serum (FBS, Cat no. 10437) were purchased from Invitrogen. The pH of RPMI-1640 and FBS was 7.3 and 7.1, respectively. The complete RPMI-1640 formulation is available online from http://www.invitrogen.com/site/us/en/home/support/Product-Technical-Resources/media_formulation.121.html. Heat inactivation of FBS was conducted by heating FBS at 55 °C for 30 min prior to use in the experiment. The NuPAGE Novex 4−12% Bis-Tris precast protein gel (Cat no. NP0322) and kit, NuPAGE 2-(*N*-morpholino) ethane sulfonic acid (MES) running buffer, NuPAGE 3-(*N*-morpholino) propane sulfonic acid (MOPS) running buffer, NuPAGE lithium dodecyl sulfate (LDS) sample buffer, and SeeBlue Plus2 protein molecular weight standard were purchased from Invitrogen. Gel code blue used for protein staining was purchased from Fisher Scientific. Low-temperature gelling agar, 2-hydroxiethyl agarose, with a gel point of <30 °C, was purchased from Sigma-Aldrich. All the chemicals were used without further purification.

Synthesis of MNPs. Magnetite nanoparticles were synthesized by coprecipitation of ferrous and ferric chloride salts in alkaline conditions as described by Kang et al.[25] Briefly, FeCl$_2$·4H$_2$O (0.01 mol) and FeCl$_3$·6H$_2$O (0.02 mol) were dissolved in HCl solution (25 mL, 0.3 M). The iron solution was added dropwise to a NaOH solution (250 mL, 1.5 M) under vigorous stirring. The magnetite synthesis was conducted in an oxygen-free environment. The black magnetite suspension was then magnetically separated and washed with N$_2$ purged Milli-Q water at least five times and suspended in 250 mL of N$_2$ purged water. The concentration of iron in the washed magnetite nanoparticles solution was measured with use of an Optima 3000D Inductive Coupled Plasma Optical Emission Spectrometer (ICP-OES).

RAFT Polymerization of Methacrylic Acid. Linear polymethacrylic acid (LPMAA20) was prepared by reversible addition−fragmentation chain transfer (RAFT) polymerization of methacrylic acid (MAA) with methanol as a solvent. 4-Cyano-4-(phenylcarbonothioylthio)pentanoic acid was used as the RAFT agent and 4,4′-azobis(4-cyanovaleric acid) was used as the radical initiator. In a small round-bottomed flask, MAA (1.7359 g, 20.2 mmol), RAFT agent (20 mg, 0.072 mmol), and radical initiator (3 mg, 0.011 mmol) were dissolved in 5 mL of methanol at a molar ratio of 280:1:0.15, respectively. The flask was sealed with a rubber septum and the mixture was purged with nitrogen for 30 min in an ice bath. The solution was then heated in an oil bath at 70 °C for 7 h. The polymerization was stopped by immersing the flask in an ice bath and exposing the solution to air. The resulting LPMAA20 was recovered and purified by repetitive precipitation in diethyl ether (150 mL), filtered, and dried under vacuum overnight. The number-average molecular weight of the resulting LPMAA20 was 20 000 Da with a polydispersity index of 1.2 as determined by nuclear magnetic resonance (NMR) and water gel permeation chromatography (GPC), respectively. Detailed characterization of LPMAA20 can be found in the Supporting Information, part A (Figures S1 and S2).

Surface Functionalization of MNPs. The surface of synthesized MNPs was functionalized with 20 kDa linear polymethacrylic acid (LPMAA20-MNPs), 25 kDa linear polyethylenimine (LPEI25-MNPs), 25 kDa branched polyethylenimine (BPEI25-MNPs), or 0.8 kDa branched oligoethylenimine (BPEI0.8-MNPs). Branched oligoethylenimine has the same structure as 25 kDa branched polyethylenimine with a significantly lower molecular weight. In all cases, a suspension of MNPs in milli-Q water (20 mL, 3 mg mL^{-1}) was prepared and sonicated for 2 min with an ultrasonic probe (Misonix Sonicator S4000) to disperse the particles. Polymer suspension (20 mL, 20 mg mL^{-1}) was then added to the sonicated MNPs solution followed by further sonication for 2 min. For the polymethacrylic acid modified MNPs, the pH was adjusted to approximately 5.5, whereas for polyethylenimine modified MNPs, the suspension pH was adjusted

to approximately 9.5; this is to aid the attachment of the polymer onto the surface of MNPs through electrostatic interaction between the oppositely charged MNPs surface and polymer at these pH values. The polymer−particle suspension was then mixed in a rotating wheel for 24 h before being washed three times in 5 mL of Milli-Q water, using magnetic separation. Washed polymer-coated MNPs were suspended in 10 mL of N_2 purged Milli-Q water. The concentrations of iron in the modified magnetite samples were determined by using an Inductive Coupled Plasma Optical Emission Spectrometer (ICP-OES).

FBS Adsorption to MNPs Surface. Adsorption of serum proteins onto the surface of bare and different functionalized MNPs was carried out by preparing MNPs (125 mg L^{-1}, based on magnetite concentration) in RPMI-1640 solution containing varying amounts of FBS or BSA, to make a total volume of 10 mL. The serum-MNPs suspension was sonicated for 30 s with an ultrasonic probe to disperse the particles, and then mixed in a rotating wheel for 24 h. Serum-free suspensions of MNPs at the same concentration were also prepared in Milli-Q water or RPMI-1640 solution for comparison.

Particle Characterization. Fourier Transform Infrared spectra of functionalized MNPs were recorded with a Perkin-Elmer Spotlight 400 FTIR spectrometer. MNPs samples were mixed with KBr and then pelletized before measurement. The specific surface area of bare MNPs was determined from Brunauer, Emmett, Teller (BET) measurements, using a Micromeritics TriStar 3000 Analyzer. Thermogravimetric analysis of MNPs samples was conducted with a Perkin-Elmer STA 6000 under a Nitrogen environment, where the temperature was first ramped to 100 °C from 25 at 40 °C min^{-1} and held at 100 °C for 5 min, followed by further ramping to 600 at 20 °C min^{-1}. The isoelectric point of various functionalized-MNPs was determined by measuring their ζ potential values in different pHs, using phase analysis light scattering (PALS, Brookhaven BI-90 PALS) where a known electric field was applied. The mobility of the particles toward an electrode of opposite charge was determined from the phase shift of an incident laser beam. The mobility was then converted to the ζ potential by application of the Smoluchowski theories.[26]

The hydrodynamic diameter of the various MNPs suspensions prepared previously was monitored by using dynamic light scattering (DLS, Brookhaven BI-90 PALS) over a period of 16 h. The samples were sonicated with an ultrasonic probe for 30 s prior to the first measurement and left undisturbed for subsequent measurements. Concurrent with the size analysis, a drop of the MNPs suspended in the various media was also deposited onto a carbon-coated copper grid and dried at room temperature for visualization under a Transmission Electron Microscope (TEM, JEOL JEM 1400) operating with an accelerating voltage of 100 kV and beam current of 55 μA.

Separation and Identification of Serum Protein Bound to MNPs by One-Dimensional (1-D) Gel Electrophoresis and Liquid Chromatograph−Mass Spectrometer/Mass Spectrometer (LC-MS/MS). Separation of serum protein bound to different types of MNPs was conducted by using 1-D sodium dodecyl sulfate−polyacrylamide gel electrophoresis (SDS-PAGE) following the method published previously,[27] using NuPAGE Novex 4−12% Bis-Tris precast protein gel, with 3-(N-morpholino) propane sulfonic acid (MOPS) as the running buffer, and a constant voltage of 170 V applied across the gel for 65 min. Gel electrophoresis was carried out in supernatant RPMI-1640 containing FBS (10 vol %) that had been in contact with MNPs, the thrice-washed supernatant solutions, and the SDS solution containing serum proteins that desorbed from the surface of FBS treated MNPs after washing. The protein gel bands of the proteins released from the washed FBS treated MNPs were cut with a clean blade and the proteins were extracted for LC-MS/MS analysis (Ultimate 3000 HPLC and autosampler system (Dionex, Amsterdam, The Netherlands) coupled with LTQ FT Ultra Mass Spectrometer (Thermo Electron, Bremen, Germany)). Reverse phase C18 material was used for the HPLC column. A detailed procedure on protein digestion and LC-MS/MS analysis were described in a previous publication.[27]

The peptide detected in the LC-MS/MS was matched with protein from the NCBInr database, using Mascot Daemon software from Matrix Science (www.matrixscience.com), with peptide mass tolerance of ±4 ppm and fragment mass tolerance of ±0.4 Da.

Quantification of Serum Protein Attracted to the Surace of MNPs. Attachment of serum protein on the surface of MNPs was quantified by using the Bradford protein assay. The concentration standard was constructed with use of bovine serum albumin (BSA), which was treated with Bradford reagent and incubated for 15 min before the absorption of the solution was read spectrophotometrically at 595 nm by a Varian Cary 300 spectrophotometer. The absorbance of supernatant FBS solution after reaction with the MNPs was measured and compared to a calibration curve using BSA as the protein standards to yield values of protein in mg mL^{-1}. The amount of protein attached was then calculated based on the amount of iron oxide core that reacted, as measured by ICP-OES.

Relaxivity Measurement. A series of particle dilutions with iron concentrations between 0 and 1.5 mM were prepared for the relaxometry measurements. Particles were suspended in water, RPMI, and RPMI with 10% FBS (or 20% FBS for the LPEI25 coated particles). Then, the suspensions were sonicated for 30 s with an ultrasonic probe to disperse the particles and then mixed in a rotating wheel for 24 h. Following this, a low-temperature gelling agar (2% w/v) was added to the samples, then the particle suspension was probed for another 30 s and transferred to NMR tubes where it was allowed to gel. Samples were then placed in an aluminum block within a water bath at 20 °C for at least 15 min before proton transverse relaxation rates were measured with a Bruker Minispec mq60 relaxometer operating at 1.4 T. A Carl-Purcell-Meiboom-Gill (CPMG) spin echo sequence was used to measure R_2, using 2000 echoes, an echo spacing of 1 ms, and a repetition time of 5 s. After the measurements, iron concentrations were verified by Inductively Coupled Plasma Atomic Emission Spectroscopy (ICP-AES) analysis after acid digestion of the samples. All samples showed a linear variation of R_2 versus concentration and therefore relaxivities (r_2) were determined from a linear fit to the data.
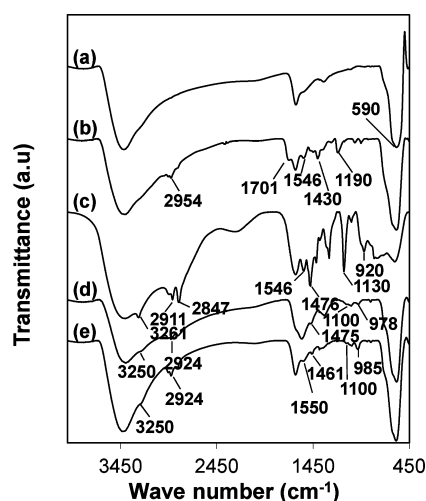
■ RESULTS AND DISCUSSION

Characteristics of Polymer-Functionalized Magnetite. The FTIR spectra in Figure 2 confirmed the presence of the polymers on the surface of the MNPs after the functionalization step. The spectrum of bare MNPs (Figure 2a) shows the characteristic Fe−O vibration band for magnetite at 587 cm^{-1}.[28]

The binding of 20 kDa linear polymethacrylic acid onto the MNPs surface resulted in the appearance of new bands at 1190, 1430, 1546, 1701, and 2954 cm^{-1} (see Figure 2b, LPMAA20-MNPs). The absorption band at 1190, 1430, and 1701 cm^{-1} can be assigned respectively to the C−O stretching, −CH_2−scissoring, and carbonyl (C=O) stretching vibrations of the adsorbed polymethacrylic acid, whereas the one at 2954 cm^{-1} can be assigned to the stretching vibrations of both −CH_2− and −CH_3. The absorption band at 1546 cm^{-1} can be attributed to the asymmetric stretching of the carboxylate ion (COO^-), and is commonly associated with iron oxide nanoparticles that have been modified with carboxylic acid functionality.[13,29]

The FTIR spectra of MNPs functionalized with ethylenimine polymers of different structures (linear or branched) and molecular weights (0.8 or 25 kDa) also showed the appearance of new bands after functionalization (see Figure 2, panels c−e, for LPEI25-MNPs, BPEI25-MNPs, and BPEI0.8-MNPs, respectively). The bands at approximately 2900 and 1460−1476 cm^{-1} are attributed to the C−H stretching vibration band and the −CH_2− scissor vibration band, respectively. The N−H stretching vibration band can be found at approximately 3250 cm^{-1}, and its deformation vibration can be found at 950 and 1550 cm^{-1}, while a slightly lower absorption band at 2850 cm^{-1}
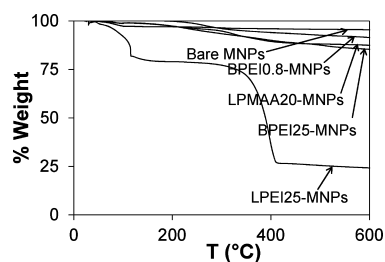
Figure 2. FTIR spectra of (a) bare magnetic nanoparticle (MNPs) and MNPs functionalized with (b) 20 kDa linear polymethacrylic acid (LPMAA20-MNPs), (c) 25 kDa linear polyethylenimine (LPEI25-MNPs), (d) 25 kDa branched polyethylenimine (BPEI25-MNPs), and (e) 0.8 kDa branched oligoethylenimine (BPEI0.8-MNPs). The table at the bottom summarizes the FTIR peak assignments for MNPs and polymer functionalized MNPs.

Sample	Peak Position (cm-1)	Peak assignment
Bare MNPs	590	Fe–O
LPMAA20-MNPs	2954	–CH2– and –CH3 stretching
	1701	–C=O stretching
	1546	COO- asymmetric stretching
	1430	–CH2– scissoring
	1190	–C–O stretching
LPEI25-MNPs	3250	N–H stretching
	2900	–CH2– stretching
BPEI25-MNPs	2850	N–C–H stretching
BPEI0.8-MNPs	1550 & 950	N–H deformation
	1460 – 1476	C–N stretching
	1100 – 1130	–CH2– scissor

is attributed to the N−C−H group. MNPs functionalized with 25 kDa linear polyethylenimine (LPEI25-MNPs) show a much stronger absorption band at approximately 1100 cm^{-1} than either of the BPEI-functionalized MNPs. This band corresponds to secondary C−N stretching vibration.[28] The strong absorption is due to the higher amount of C−N bond on the surface, which is an indication of the higher amount of linear polyethylenimine adsorbed on the MNPs surface compared to branched polyethylenimine.

Thermogravimetric analysis curves in Figure 3 showed the mass percent composition of each polymer in the functionalized MNPs. The bare MNPs showed a weight loss of 4.5%, which is attributed to the loss of residual adsorbed water at approximately 100 °C. The functionalized MNPs showed further weight loss at over 300 °C due to degradation of polymer, which indicates the weight percent of the polymer coating in the modified MNPs. For MNPs functionalized with 20 kDa linear polymethacrylic acid (LPMAA20-MNPs), 25 kDa

Sample	% wt Polymer
Bare MNPs	0
LPMAA20-MNPs	11
LPEI25-MNPs	56
BPEI25-MNPs	13
BPEI0.8-MNPs	11

Figure 3. Thermogravimetric analysis curves obtained from heating bare MNPs and MNPs functionalized with 20 kDa linear polymethacrylic acid (LPMAA20-MNPs), 25 kDa linear polyethylenimine (LPEI25-MNPs), 25 kDa branched polyethylenimine (BPEI25-MNPs), and 0.8 kDa branched oligoethylenimine (BPEI0.8-MNPs) from 25 to 600 °C in an oxygen-free environment. The table at the bottom summarizes the weight percent of polymer in functionalized MNPs after deduction with the amount of water content that is lost after heating to approximately 100 °C.

branched polyethylenimine (BPEI25-MNPs) and 0.8 kDa branched oligoethylenimine (BPEI0.8-MNPs), the polymer composition was less than 15%. For MNPs functionalized with 25 kDa linear polyethylenimine (LPEI25-MNPs), a sharp decrease in weight was observed, which corresponds to the higher amount of polymer adsorbed of approximately 56%; this indicates that a greater amount of linear PEI was adsorbed onto the MNPs surface compared to the other polymers. The polymer coverage on the surface of MNPs can be estimated based on these results and the measured surface area of MNPs (120 m^2/g), as shown in the Supporting Information, part C. We found that the amount of LPMAA20, LPEI25, BPEI25, and LPEI25 on MNPs surface is 0.03, 0.26, 0.03, and 0.78 molecules/nm^2, respectively.

Figure 4 shows the ζ potential values of the bare and functionalized MNPs across different pH values. In general, the bare and polymer functionalized MNPs have positive ζ potential at a low pH and negative ζ potential at a high pH. A shift in the isoelectric point (pI) from 7.8 to 3.5 was observed after the bare MNPs were functionalized with linear polymethacrylic acid (LPMAA20-MNPs), and from 7.8 to 11.5 and 10 after functionalization with 25 kDa linear and branched polyethylenimine (LPEI25-MNPs and BPEI25-MNPs), and branched oligoethylenimine (BPEI0.8-MNPs), respectively.

Linear polymethacrylic acid consists of a single chain polymer with pendant carboxylic acid groups on the polymer backbone. Previous investigations have shown that at pH values similar to the pK_a of polymethacrylic acid (pK_a = 5.98), polymer binding to the MNPs surface occurs via hydrogen bonding between undissociated carboxylic groups (−COOH) on the polymer and protonated surface hydroxyl species (Fe−OH$_2^+$) on the MNPs surface.[30] Some degree of polymer adsorption also occurs via electrostatic interaction between −Fe−OH$_2^+$ and dissociated carboxylic groups on the polymer (−COO$^-$). The drop in ζ potential of the MNPs after
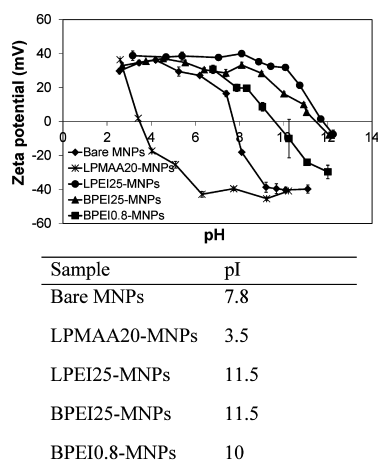
Figure 4. The ζ potential curves and isoelectric points of bare MNPs and MNPs functionalized with 20 kDa polymethacrylic acid (LPMAA20-MNPs), 25 kDa linear polyethylenimine (LPEI25-MNPs), 25 kDa branched polyethylenimine (BPEI25-MNPs), and 0.8 kDa branched oligoethylenimine (BPEI0.8-MNPs) suspended in 1.5 mM NaCl solution. The table at the bottom summarizes the isoelectric points of the MNPs and polymer functionalized MNPs as determined from the interception of the ζ potential curves with the x-axis.

functionalization with polymethacrylic acid can be attributed to the dissociation of the carboxylic groups to form COO^-. At the higher pH, the degree of dissociation of polymethacrylic acid increases; likewise, the deprotonation of $-Fe-OH_2^+$ species on the MNPs surface to form $-Fe-OH$ and $-Fe-O^-$ also increases. This results in a shift of the ζ potential toward increasingly negative values at high pH.

Linear polyethylenimine consists of a single chain polymer with secondary amine groups on the polymer backbone. Branched PEI, in contrast, consists of primary, secondary, and tertiary amines at a 1:2:1 molar ratio, respectively. Chibowski et al. showed that binding between the ethylenimine polymer and hematite surfaces at pH ~9 occurs when positively charged amine groups cause hydrogen ions to dissociate from surface hydroxyl groups ($-Fe-OH$).[30] As a result, a large number of $-FeO^-$ species are formed, upon which the polyethylenimine can be adsorbed. A similar binding mechanism is thought to occur between polyethylenimine and MNPs. The increase in ζ potential of the MNPs after functionalization with polyethylenimine is due to the presence of positively charged amine groups ($-NH_3^+$, $=NH_2^+$, or $\equiv NH^+$). With an increase in pH, deprotonation of the amine and surface hydroxyl groups increases, and as a result, the ζ potential becomes increasingly negative as the pH increases.

In our study, the ζ potential analysis also found that BPEI0.8-MNPs had a lower pI (approximately 10) than BPEI25-MNPs and LPEI25-MNPs (pI = 11.5). TGA further showed that the weight percent of branched oligoethylenimine on the MNPs surface was similar to that of 25 kDa branched polyethylenimine in BPEI25-MNPs. We note here that both low and high molecular weight branched polyethylenimine contain the same ratio of primary, secondary, and tertiary amine groups (approximately 1:2:1); branch size is also very similar, but chain length and number of branching points increased with increasing molecular weight. Since the surface area available for binding is the same, we can expect higher molecular weight polymers taking on a more spatial conformation of loops and

tail than low molecular weight polymers (see Figure 5). Hence, the influence of nonbonded amine groups is greater, which
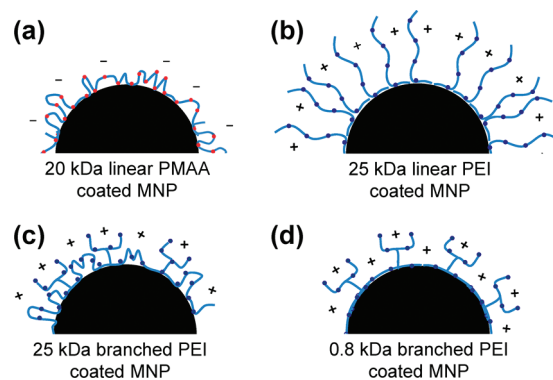

Figure 5. Schematic figure showing anticipated conformation of the polymers on the MNPs surface for MNPs functionalized with (a) 20 kDa polymethacrylic acid (LPMAA20-MNPs), (b) 25 kDa linear polyethylenimine (LPEI25-MNPs), (c) 25 kDa branched polyethylenimine (BPEI25-MNPs), and (d) 0.8 kDa branched oligoethylenimine (BPEI0.8-MNPs). Red dots represent the carboxylic acid groups and blue dots represent amine groups.

explains the higher pI for MNPs functionalized with higher molecular weight polyethylenimine. A similar observation was made by Madigan et al. for goethite particles coated with polyethylenimine.[31]

Another interesting pattern emerging from the FTIR and TGA measurements is that the amount of linear polyethylenimine adsorbed onto the MNPs is significantly greater than that of the other polymers, including branched polyethylenimine with the same molecular weight (MW = 25 kDa). This observation can be explained by the weaker linear charge of the linear polyethylenimine polymer (pK_b = 7.9) compared to that of branched polyethylenimine (pK_b = 8.8).[32] As such, a smaller segment of the linear polyethylenimine polymer will actually interact and bind with the MNPs, with the remaining portion of the polymer forming loops and tails that extend into the bulk solution (see Figure 5).

Protein Adsorption onto Bare and Polymer-Functionalized MNPs. Transmission Electron Microscopy (TEM) images of bare MNPs and MNPs functionalized with 20 kDa polymethacrylic acid (LPMAA20-MNPs), 25 kDa linear polyethylenimine (LPEI25-MNPs), 25 kDa branched polyethylenimine (BPEI25-MNPs), and 0.8 kDa branched oligoethylenimine (BPEI0.8-MNPs) are shown in Figure 6. The TEM images show that the synthesized MNPs have a primary particle size of approximately 10 to 20 nm, which is comparable to reported values in the literature.[33,34]

The images also show that when the bare and polymer functionalized MNPs were suspended in serum-free RPMI-1640 solution, they formed large and extensive aggregates in the micrometer size range (Figure 6, top panel). When the MNPs were suspended in RPMI-1640 containing FBS, a thick protein corona encapsulated the MNPs (Figure 6, middle panel). The size of the bare and functionalized MNPs aggregates also appeared to have decreased to approximately 200−300 nm. Following contact between the MNPs samples and FBS, the MNPs were thrice-washed (with water), and then resuspended in serum-free RPMI-1640 solution. The presence of a thick protein corona was no longer visible and the size of
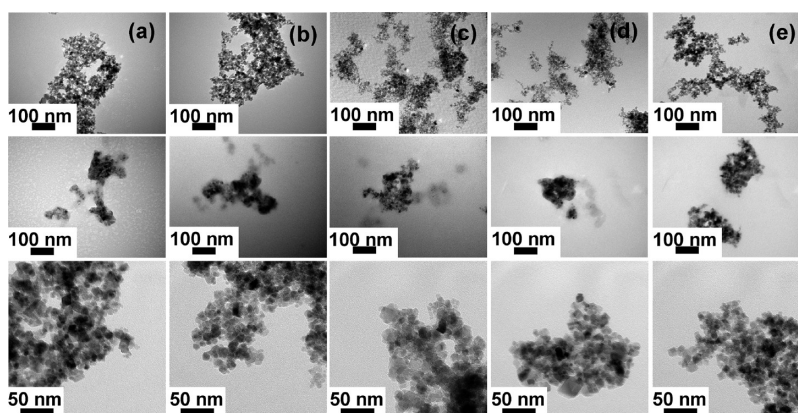
Figure 6. Transmission Electron Microscopy images of (a) bare MNPs and MNPs functionalized with (b) 20 kDa linear polymethacrylic acid (LPMAA20-MNPs), (c) 25 kDa linear polyethylenimine (LPEI25-MNPs), (d) 25 kDa branched polyethylenimine (BPEI25-MNPs), and (e) 0.8 kDa branched oligoethylenimine (BPEI0.8-MNPs). MNPs were suspended in serum-free RPMI-1640 cell culture media (top panel) and in RPMI-1640 containing 10% FBS, except for LEPI25-MNPs, which contained 20% FBS (middle panel). MNPs samples that were collected after being suspended in FBS, washed and then resuspended in serum-free RPMI-1640 are also shown (bottom panel). Scale bars represent 100 nm for top and middle panels and 50 nm for bottom panels.
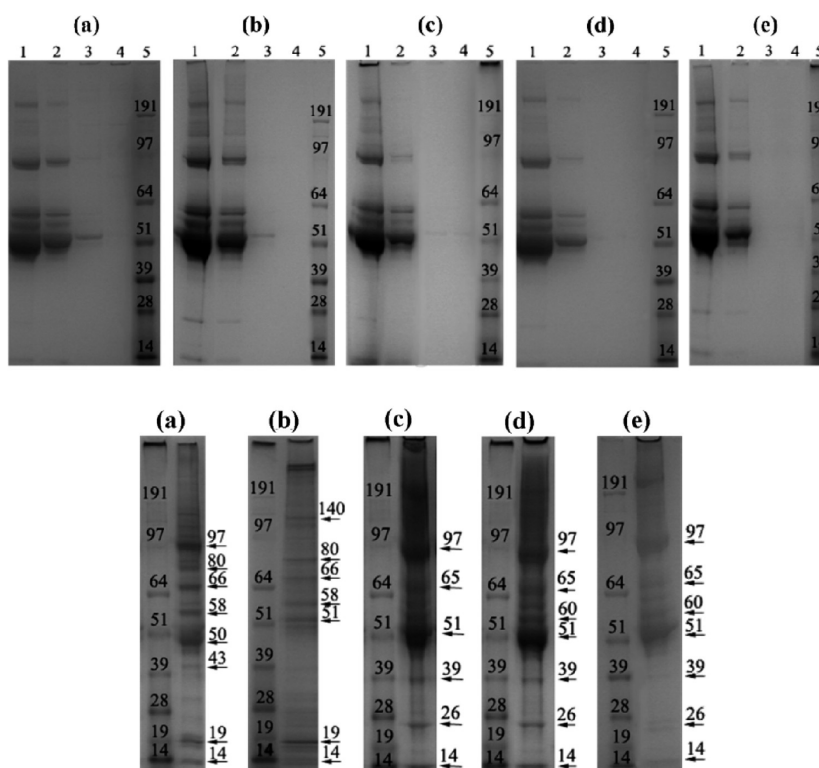

Figure 7. Protein bands produced from the 1-D gel electrophoresis of FBS proteins with low (top) and high (bottom) affinity for the surface of (a) bare MNPs and MNPs functionalized with (b) 20 kDa polymethacrylic acid (LPMAA20-MNPs), (c) 25 kDa linear polyethylenimine (LPEI25-MNPs), (d) 25 kDa branched polyethylenimine (BPEI25-MNPs), and (e) 0.8 kDa branched oligoethylenimine (BPEI0.8-MNPs). The MNPs have been contacted with biological solution containing 10% FBS prior to the analysis. In the top panel, lane 1 shows the bands of proteins which remain in the solution after contact with MNPs; lanes 2, 3, and 4 show the bands of proteins which were released from the surface of the MNPs after 1, 2, and 3 cycles of washing, respectively; lane 5 shows the bands of the molecular weight marker. The bottom panel shows the bands of high affinity proteins which remain on the surface MNPs after three cycles of washing, with the left lane showing the bands of the molecular weight marker.

the MNPs aggregates reverted back to the micrometer size range (Figure 6, bottom panel).

The removal of adsorbed protein by the washing is confirmed by 1-D gel electrophoresis of the wash solution. Figure 7 (top) shows that most of the proteins detached in the first wash cycle, and no more protein was removed from the MNPs surfaces after three wash cycles. More interestingly, Figure 7 (bottom) also reveals the presence of strongly

attached proteins on the MNPs surfaces after three wash cycles, despite the fact that no proteins were detected in the wash solution and no protein corona was visible under TEM (Figure 6, bottom panel). Control experiments where different MNPs were suspended in serum-free RPMI-1640 did not produce any protein bands (see the Supporting Information, part B, Figure S3); this confirms that the proteins that were adsorbed and released from the MNPs originated from FBS.

The intensity of the protein bands is indicative of the amount of protein. That is, the darker the band, the greater the amount of proteins present in the wash solutions or MNPs surfaces. Figure 7 shows that BPEI25-MNPs produced the darkest bands for the leached proteins and the lightest bands for the wash solution. This indicates that BPEI25-MNPs retain more adsorbed proteins on their surface than the other MNPs samples. In contrast, LPMAA20-MNPs showed the lightest bands for the leached proteins and the darkest bands for the wash solution, indicating that polymethacrylic acid functionalized MNPs were the least likely to retain the protein molecules on its surface.

The amount of protein adsorbed by each polymer functionalized MNPs was further quantified by measuring the change in FBS protein concentration in a RPMI-1640 solution from an initial value of 0.5% FBS following contact with MNPs. Figure 8 shows that BPEI25-MNPs adsorbed the most FBS protein at 0.07 ± 0.01 mg protein per mg MNPs. Bare MNPs and BPEI0.8-MNPs adsorbed approximately 0.05 ± 0.01 mg
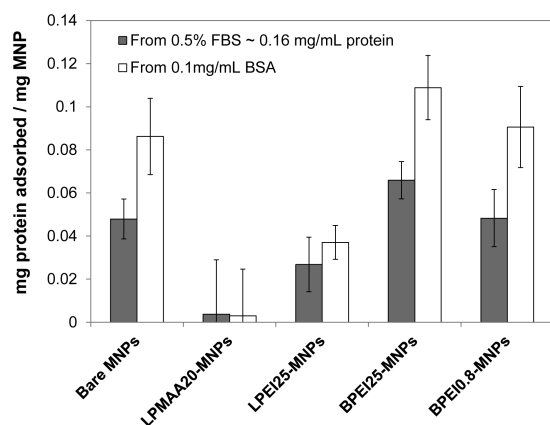

Figure 8. Amount of FBS protein or BSA adsorbed onto the surface of bare MNPs and MNPs functionalized with 20 kDa polymethacrylic acid (LPMAA20-MNPs), 25 kDa linear polyethylenimine (LPEI25-MNPs), 25 kDa branched polyethylenimine (BPEI25-MNPs), and 0.8 kDa branched oligoethylenimine (BPEI0.8-MNPs) after being contacted with RPMI-1640 solution containing 0.5% FBS (equivalent to 0.16 mg/mL protein) or 0.1 mg/mL BSA.

protein per mg MNPs, while LPEI25-MNPs adsorbed approximately 0.03 ± 0.01 mg protein per mg MNPs. The LPMAA20-MNPs, in contrast, adsorbed only a small amount of protein (0.004 ± 0.02 mg per mg MNPs). A similar trend in protein adsorption capacity was found for the bare and polymer functionalized MNPs that were treated in the same manner with bovine serum albumin (BSA) in place of FBS (see Figure 8).

The proteins that remained on the surface of each polymer functionalized MNPs after three wash cycles were identified by LC-MS/MS and are shown in Table 1. The molecular weight of each protein (determined in the gel electrophoresis studies) and theoretical isoelectric point of the protein (from ExPASy database, http://web.expasy.org/compute_pi/) are listed alongside. From Table 1 it is clear that a range of proteins remain on the MNPs surfaces after washing; these proteins have isoelectric points between 4.6 and 8.7, and molecular weights ranging from 14 to 140 kDa.

Proteins which are strongly adsorbed and retained on positively charged polyethylenimine functionalized MNPs

(LPEI25-MNPs and BPEI25-MNPs) have acidic isoelectric points (pI < 7), whereas those that adsorbed onto bare and negatively charged linear polymethacrylic acid functionalized MNPs (LPMAA20-MNPs) tended to have basic isoelectric points (pI > 7). Moreover, MNPs that were functionalized with polyethylenimine attracted similar types of proteins, regardless of whether the polymer was branched or linear. The only difference between branched or linear was three additional proteins—antithrombin, α-fetoprotein and α-1-antiproteinase—which were detected on the surface of MNPs functionalized with branched polyethylenimine. Albumin and hemoglobin adsorbed onto all four MNPs samples.

The gel-electrophoresis and protein adsorption studies provided insights into the mechanisms and factors governing the adsorption of protein molecules onto polymer functionalized MNPs. Notably, they showed that the amount of protein adsorbed and retained on the MNPs surfaces after washing is greatly dependent on the charge difference between the surface of functionalized MNPs and the protein, i.e. negatively charged proteins are more likely to be adsorbed and retained on a positively charged MNPs surfaces. This was expected and confirms previous literature reports. The study by Gessner et al., for instance, showed the preferential binding of protein with a pI greater than 5.5 onto acidic surfaces, while proteins with a pI of less than 5.5 have greater affinity for basic surfaces.[35] It is, however, noteworthy that the adsorption of protein onto the MNPs surfaces is not solely driven by electrostatic factors. Table 1 shows that MNPs that were functionalized with negatively charged polymethacrylic acid can still attract negatively charged proteins. This is due to the intrinsic amphiphilic character of the protein that facilitated the adsorption of protein onto similarly charged surfaces.[36] Hence, although the net charge of a protein is negative, positively charged patches on the protein surface are also present due to the heterogeneous distribution on the protein surface.[37,38] Park et al. demonstrated positive charge patches in bovine serum albumin (BSA) (that is otherwise negatively charged),[39] allowing BSA to bind with a strong polyanion, as also observed in this work and in a previous report.[32,38] The protein could also carry multiple positive charges and therefore be able to replace the counterions on a polymer surface.[32,36] In addition, albumin can also bind to the hydrophobic site of polymethacrylic acid. The binding between albumin and a hydrophobic surface is often used as a protein carrier for hydrophobic molecules, such as drugs.[40]

MNPs functionalized with branched polyethylenimine also adsorbed and retained more protein than linear polyethylenimine functionalized MNPs. The MNPs coated with higher molecular weight branched ethylenimine polymer also appeared to adsorb and retain a greater amount of protein than MNPs coated with lower molecular weight polymers. This suggests that in addition to surface charge, the polymer architecture and molecular weight can also influence the interactions of proteins with the polymer functionalized MNPs. Branched polyethylenimine functionalized MNPs, particularly ones with a higher molecular weight (BPEI25-MNPs), adsorbs and retains more protein due to the fact that there is a greater number of nonbonded branching points and more loops conformation of the polymer on the MNPs surface.

Effects of the Type and Amount of Protein Adsorbed on the Biological Function of Magnetic Nanoparticles. Dynamic Light Scattering measurements show the aggregate size of polymer functionalized MNPs can be maintained below

Table 1. LC-MS/MS Analysis of FBS Proteins That Remain on the Surface of Bare MNPs and MNPs Functionalized with 20 kDa Polymethacrylic Acid (LPMAA20-MNPs), 25 kDa Linear Polyethylenimine (LPEI25-MNPs), and 25 kDa Branched Polyethylenimine (BPEI25-MNPs) after MNPs Have Been Contacted with Biological Solution Containing 10% FBS and Then Washed Thrice with Water

protein	MW (kDa)	pI[a]	bare MNPs	LPMAA20-MNPs	LPEI25-MNPs	BPEI25-MNPs
albumin	50	4.6	√	√	√	√
antithrombin	51	4.6				√
α-2-HS-glycoprotein	43	5.1	√			
inter-α-inhibitor	97	5.2			√	√
apolipoprotein A-1	28	5.4			√	√
apolipoprotein E	39	5.4			√	√
complement component 4A	65	5.6			√	√
tetranectin	19	5.7	√	√		
α-fetoprotein	60	5.9				√
α-1-antiproteinase	60	6.0				√
kininogen	80	6.1		√		
complement factor H	97	6.3	√			
hemoglobin	14	6.5	√	√	√	√
immunoglobulin	140	7.0		√		
complement factor I	66	7.4	√			
complement factor B	58	7.7	√	√		
apolipoprotein B	80	8.0	√			
lactoferrin	66	8.7		√		

[a]Isoelectric point (pI) of protein determined theoretically from the amino acid sequence of protein (http://web.expasy.org/compute_pi/).

300 nm for at least 16 h in water at pH 7.4 (Supporting Information, part D, Figure S4), while unmodified MNPs aggregated to over 1 μm within 1 h of measurement. The observed stability of the polymer functionalized MNPs in water is due to the highly positively charged polyethylenimine modified MNPs and highly negatively charged polymethacrylic acid modified MNPs, which induces a strong electrostatic repulsion between the particles. In addition, the polymer coating also provides a steric hindrance to increase distance between particles and hence reduces the strength of magnetic interactions.[41,42]

Despite the presence of a highly positively charged amine group or a highly negatively charged carboxylic acid group on its surface, the functionalized MNPs could not remain as stable aggregates in cell culture media (RPMI-1640) shown by Figure 9, confirming TEM images previously shown by Figure 6 (top panel). DLS measurements for the polymer functionalized MNPs showed a shift in the intensity weighted distribution of the particles toward a larger size distribution after just 1 h, consistent with the formation of micrometer size aggregates as shown in the Supporting Information (part D, Figure S5). The high ionic strength of RPMI-1640 media suppresses the charge introduced by amine and carboxyl groups, therefore reducing the electrostatic repulsion between the particles and decreasing the colloidal stability of MNPs.

When both the bare and functionalized MNPs were transferred into RPMI-1640 solution containing varying amounts of FBS, we found that the aggregation behavior was again altered, resulting in stable aggregates with hydrodynamic diameter of approximately 250 nm (Figure 9a−e, intensity weighted distribution is shown in the Supporting Information, part D, Figure S6), also confirming the observation from TEM images shown by Figure 6 (middle panel). Although the size of MNP aggregates is larger than the optimal particle size preferred for in vivo application, prevention from further aggregation in RPMI-1640 solution (a challenging problem of MNPs in high ionic strength solution) demonstrates the

possibility of the application of these MNPs in vivo as well as in vitro. Moreover, we found that depending on the type of surface functional group that was present on the particles' surface, the amount of FBS required to stabilize the bare and functionalized MNPs in RPMI-1640 differed. The highest amount of FBS was required by LPEI25-MNPs at 20% FBS, followed by LPMAA20-MNPs at 6% FBS, bare MNPs at 2% FBS, BPEI0.8-MNPs at 1% FBS, and finally by BPEI25-MNPs at 0.5% FBS. A DLS study further showed that the aggregation stability is lost when the polymer functionalized MNPs are washed and then resuspended in serum free RPMI-1640 solution, although the aggregation rate is slower compared to that of the MNPs that have never been contacted with FBS (Figure 9f).

We have previously shown that a soft/hard protein corona formed when carboxyl-coated MNPs were incubated in RPMI-1640 containing an excess amount of FBS. A group of irreversible adsorbed proteins, known as hard corona, bind a second set of lower affinity proteins, known as the soft corona, to the surface of the MNPs. The soft protein corona was shown to be the responsible factor for the aggregation stability of nanoparticles, as stability could not be maintained when the soft corona was removed.[27] In the present work, the stabilizing effect of FBS on the bare and polymer functionalized MNPs suspended in biological fluid can be attributed to a similar mechanism.

In general, the results show that an increase in protein attracted by the MNPs surfaces improves size stability of the magnetic nanoparticle aggregates. The only exception to this is the MNPs that were functionalized with linear polyethylenimine (LPEI25-MNPs). A possible explanation for this is that linear polyethylenimine does not bind as well as the other polymers to the MNPs surface. Hence, a significant proportion of the polymer exists as loops and tails that extend from the MNPs surface to the bulk solution. This type of polymer conformation predisposes the MNPs to aggregation induced by polymer bridging.
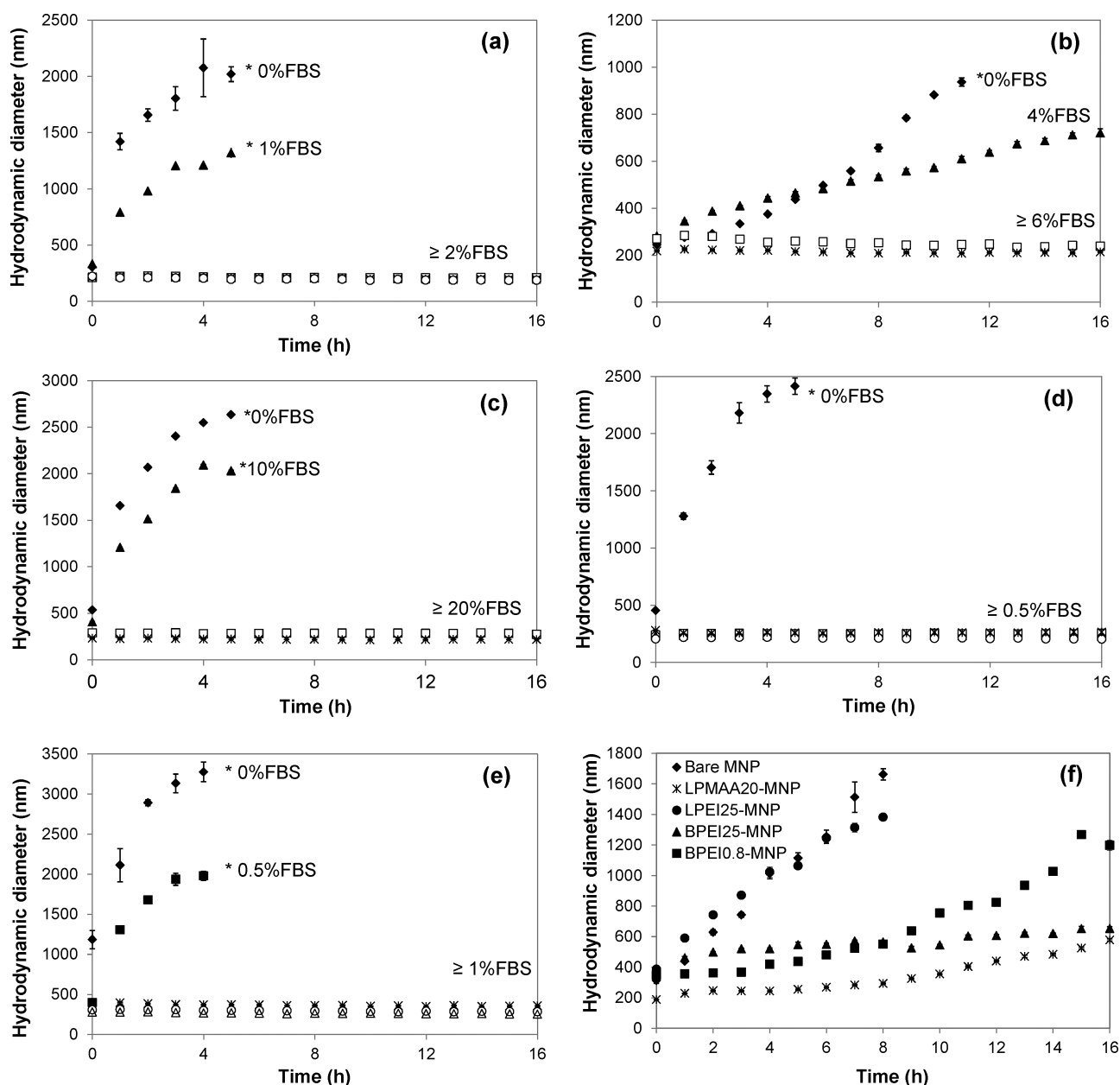
Figure 9. Light scattering average hydrodynamic diameter of (a) bare MNPs and MNPs functionalized with (b) 20 kDa polymethacrylic acid (LPMAA20-MNPs), (c) 25 kDa linear polyethylenimine (LPEI25-MNPs), (d) 25 kDa branched polyethylenimine (BPEI25-MNPs), (e) 0.8 kDa branched oligoethylenimine (BPEI0.8-MNPs) suspended in biological media containing different amounts of fetal bovine serum (FBS), and (f) washed FBS treated MNPs resuspended in FBS-free RPMI-1640. An asterisk indicates measurements were not continued for a longer period.

The change in aggregation stability can have a significant impact on the biological function of the MNPs. Here we show that protein adsorption results in a change in the relaxivity of MNPs, which determine their quality as MRI contrast agents. Figure 10 shows the r_2 relaxivity values of bare MNPs and polymer functionalized MNPs in water and RPMI-1640 solution containing FBS. The relaxivity for the protein-coated samples in RPMI was generally lower than that for the same samples suspended in water. This apparent decrease in relaxivity of the particles when coated with proteins is likely due to a change in the size of aggregates in solution. The protein-coated particles generally have smaller aggregates (see the Supporting Information, part D, Figure S7); previous studies have demonstrated that the size and volume fraction of

aggregates is a significant factor in determining the relaxivity values of iron oxide based nanoparticulate contrast agents.[43,44]

The transverse relaxivities for most of the protein-coated particles are similar to those of commercial contrast agents[45] and in some cases the relaxivities are significantly higher. Hence, these particles should provide good contrast in T2 weighted MRI images. This work shows that interaction with serum proteins has a significant effect on the magnitude of the transverse relaxivities of the MNPs and hence such interactions should be considered during the development of iron oxide based contrast agents. Indeed for the development of more advanced applications such as quantitative molecular imaging, the interactions between the contrast agents and biological system require significant additional investigations.
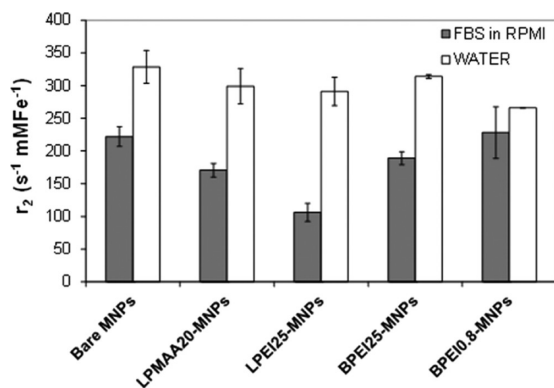
Figure 10. Relaxivity r_2 of bare MNPs and MNPs functionalized with linear 20 kDa polymethacrylic acid (LPMAA20-MNPs), 25 kDa linear polyethylenimine (LPEI25-MNPs), 25 kDa branched polyethylenimine (BPEI25-MNPs), and 0.8 kDa branched oligoethylenimine (BPEI0.8-MNPs) in water and RPMI-1640 containing FBS under 1.4 T applied field.

CONCLUSION

This study showed that polymers with different functional groups, architecture, and molecular weight have different conformations when bound to the surface of MNPs. This, in turn, affects the biological serum protein interaction with the surface of bare and functionalized MNPs to form a protein corona surrounding the particles. MNPs coated with 25 kDa branched polyethylenimine were found to attract the highest amount of serum protein, followed by similar adsorption by the bare MNPs and those coated with 0.8 kDa branched oligoethylenimine. MNPs coated with linear polyethylenimine of high molecular weight adsorbed less protein; MNPs coated with 20 kDa linear polymethacrylic acid adsorbed the least amount of protein. Different protein interactions with different MNPs surfaces affected the aggregate stability of MNPs in the biological media, RPMI-1640. Generally, MNPs that adsorbed more protein could be stabilized in RPMI-1640 with lower amounts of serum protein. However, MNPs functionalized with 25 kDa linear polyethylenimine required the highest amount of serum for particle stability despite the large amounts of adsorbed protein. This is due to the conformation of the polymer on the surface of the MNPs, with most of the polymer chain being extended in solution and thus requiring a higher amount of protein to prevent aggregation due to polymer bridging. The effect of serum protein on the size of particles was also shown to cause a reduction on the r_2 relaxivity of particles, which is an important characteristic of MNPs as MRI contrast agents.

This study provides a better understanding of the formation of protein corona on MNPs functionalized with different types, architecture, and molecular weight polymers. The impact of the protein corona formation on the particles' size and its subsequent effect on the function of these MNPs as potential MRI contrast agents is presented. It has clearly demonstrated the importance of simulating biological conditions to study and explore the potential of magnetic nanoparticles for biological applications due to the unavoidable contact and interaction between the particles and the biological environment.

ASSOCIATED CONTENT

S **Supporting Information**

Characterization of RAFT polymethacrylic acid and more detailed characterization of the bare and functionalized nanoparticles are provided via DLS and gel electrophoresis analysis. This information is available free of charge via the Internet at http://pubs.acs.org/.

AUTHOR INFORMATION

Corresponding Author

*Tel.: +6129385 4361, Fax: +6129385 5966, E-mail: r.amal@unsw.edu.au.

Notes

The authors declare no competing financial interest.

ACKNOWLEDGMENTS

REFERENCES

(1) Nitin, N.; LaConte, L.; Zurkiya, O.; Hu, X.; Bao, G. *J. Biol. Inorg. Chem.* **2004**, *9* (6), 706−712.

(2) Reza, R. T.; Martínez Pérez, C. A.; Rodríguez González, C. A.; Romero, H. M.; García Casillas, P. E. *Cent. Eur. J. Chem.* **2010**, *8* (5), 1041−1046.

(3) Gupta, A. K.; Gupta, M. *Biomaterials* **2005**, *26* (18), 3995−4021.

(4) Goon, I. Y.; Lai, L. M. H.; Lim, M.; Amal, R.; Gooding, J. J. *Chem. Commun.* **2010**, *46*, 8821−8823.

(5) Fukumori, Y.; Ichikawa, H. *Adv. Powder Technol.* **2006**, *17* (1), 1−28.

(6) Arsianti, M.; Lim, M.; Marquis, C. P.; Amal, R. *Langmuir* **2010**, *26* (10), 7314−7326.

(7) Neuberger, T.; Schöpf, B.; Hofmann, H.; Hofmann, M.; Von Rechenberg, B. *J. Magn. Magn. Mater.* **2005**, *293* (1), 483−496.

(8) Moghimi, S. M.; Hunter, A. C.; Murray, J. C. *FASEB J.* **2005**, *19* (3), 311.

(9) Longmire, M.; Choyke, P. L.; Kobayashi, H. *Nanomedicine* **2008**, *3* (5), 703−717.

(10) Horak, D.; Babi, M.; Mackova, H.; Beneš, M. J. *J. Sep. Sci.* **2007**, *30* (11), 1751−1772.

(11) Boyer, C.; Whittaker, M. R.; Bulmus, V.; Liu, J.; Davis, T. P. *NPG Asia Materials* **2010**, *2* (1), 23−30.

(12) Liu, Z.; Liu, C.; Yao, K.; Liu, P.; Ning, Q. *J. Appl. Polym. Sci.* **2007**, *105* (3), 1331−1335.

(13) Tural, B.; Kaya, M.; Ozkan, N.; Volkan, M. *J. Nanosci. Nanotechnol.* **2008**, *8* (2), 695−701.

(14) Ko, Y. T.; Kale, A.; Hartner, W. C.; Papahadjopoulos-Sternberg, B.; Torchilin, V. P. *J. Controlled Release* **2009**, *133* (2), 132−138.

(15) Arsianti, M.; Lim, M.; Marquis, C. P.; Amal, R. *Biomacromolecules* **2010**, *11* (9), 2521−2531.

(16) Lee, S. Y.; Huh, M. S.; Lee, S.; Lee, S. J.; Chung, H.; Park, J. H.; Oh, Y. K.; Choi, K.; Kim, K.; Kwon, I. C. *J. Controlled Release* **2010**, *141* (3), 339−346.

(17) Nel, A. E.; Mädler, L.; Velegol, D.; Xia, T.; Hoek, E. M. V.; Somasundaran, P.; Klaessig, F.; Castranova, V.; Thompson, M. *Nat. Mater.* **2009**, *8* (7), 543−557.

(18) Eberbeck, D.; Kettering, M.; Bergemann, C.; Zirpel, P.; Hilger, I.; Trahms, L. *J. Phys. D: Appl. Phys.* **2010**, *43*, 405002.

(19) Lundqvist, M.; Sethson, I.; Jonsson, B. H. *Langmuir* **2004**, *20* (24), 10639−10647.

(20) Mu, Q.; Li, Z.; Li, X.; Mishra, S. R.; Zhang, B.; Si, Z.; Yang, L.; Jiang, W.; Yan, B. *J. Phys. Chem. C.* **2009**, *113* (14), 5390−5395.

(21) Nel, A.; Xia, T.; Mädler, L.; Li, N. *Science* **2006**, *311* (5761), 622.

(22) Petri-Fink, A.; Steitz, B.; Finka, A.; Salaklang, J.; Hofmann, H. *Eur. J. Pharm. Biopharm.* **2008**, *68* (1), 129−137.

(23) Shang, W.; Nuffer, J. H.; Muñiz Papandrea, V. A.; Colón, W.; Siegel, R. W.; Dordick, J. S. *Small* **2009**, *5* (4), 470−476.

(24) Vertegel, A. A.; Siegel, R. W.; Dordick, J. S. *Langmuir* **2004**, *20* (16), 6800−6807.

(25) Kang, Y. S.; Risbud, S.; Rabolt, J. F.; Stroeve, P. *Chem. Mater.* **1996**, *8* (9), 2209−2211.

(26) McNeil-Watson, F.; Tscharnuter, W.; Miller, J. *Colloids Surf., A* **1998**, *140* (1−3), 53−57.

(27) Wiogo, H. T. R.; Lim, M.; Bulmus, V.; Yun, J.; Amal, R. *Langmuir* **2011**, *27* (2), 843−850.

(28) Xu, L.; Yang, L.; Luo, M.; Liang, X.; Wei, X.; Zhao, J.; Liu, H. *J. Hazard. Mater.* **2011**, *189* (3), 787−793.

(29) Kataby, G.; Cojocaru, M.; Prozorov, R.; Gedanken, A. *Langmuir* **1999**, *15* (5), 1703−1708.

(30) Chibowski, S.; Patkowski, J.; Grzadka, E. *J. Colloid Interface Sci.* **2009**, *329* (1), 1−10.

(31) Madigan, C.; Leong, Y.; Ong, B. *Int. J. Miner. Process.* **2009**, *93* (1), 41−47.

(32) Erol, M.; Du, H.; Sukhishvili, S. *Langmuir* **2006**, *22* (26), 11329−11336.

(33) Cornell, R. M.; Schwertmann, U. *The iron oxides: Structure, properties, reactions, occurrences, and uses*; WILEY-VCH Verlag GmbH & Co KGaA: Weinham, Germany, 2003.

(34) Rodríguez, J. A.; Garcia, M. F. *Synthesis, properties, and applications of oxide nanomaterials*; John Wiley & Sons: Hoboken, NJ, 2007.

(35) Gessner, A.; Lieske, A.; Paulke, B. R.; Müller, R. H. *J. Biomed. Mater. Res., Part A* **2003**, *65* (3), 319−326.

(36) Wittemann, A.; Ballauff, M. *Phys. Chem. Chem. Phys.* **2006**, *8* (45), 5269−5275.

(37) Patel, N.; Davies, M. C.; Hartshorne, M.; Heaton, R. J.; Roberts, C. J.; Tendler, S. J. B.; Williams, P. M. *Langmuir* **1997**, *13* (24), 6485−6490.

(38) Seyrek, E.; Dubin, P. L.; Tribet, C.; Gamble, E. A. *Biomacromolecules* **2003**, *4* (2), 273−282.

(39) Park, J. M.; Muhoberac, B. B.; Dubin, P. L.; Xia, J. *Macromolecules* **1992**, *25* (1), 290−295.

(40) Kratz, F. *J. Controlled Release* **2008**, *132* (3), 171−183.

(41) Mefford, O. T.; Vadala, M. L.; Goff, J. D.; Carroll, M. R. J.; Mejia-Ariza, R.; Caba, B. L.; Pierre, T. G. S.; Woodward, R. C.; Davis, R. M.; Riffle, J. *Langmuir* **2008**, *24* (9), 5060−5069.

(42) Ramanujan, R. V.; Chong, W. T. *J. Mater. Sci.: Mater. Med.* **2004**, *15* (8), 901−908.

(43) Carroll, M. R. J.; Huffstetler, P. P.; Miles, W. C.; Goff, J. D.; Davis, R. M.; Riffle, J. S.; House, M. J.; Woodward, R. C.; St Pierre, T. G. *Nanotechnology* **2011**, *22*, 325702.

(44) Carroll, M. R. J.; Woodward, R. C.; House, M. J.; Teoh, W. Y.; Amal, R.; Hanley, T. L.; St Pierre, T. G. *Nanotechnology* **2010**, *21*, 035103.

(45) Masotti, A.; Pitta, A.; Ortaggi, G.; Corti, M.; Innocenti, C.; Lascialfari, A.; Marinone, M.; Marzola, P.; Daducci, A.; Sbarbati, A. *Magn. Reson. Mater. Phys., Biol. Med.* **2009**, *22* (2), 77−87.